Electronic Supplementary Material (ESI) for Communications.

Electronic Supplementary Information

Doping-Modulated Water Dissociation for Energy-Efficient Hydrogen Production

Dongxing Tan,[a]* Shuangfeng Li,[a] Hengrui Kang,[a] Ruize Li,[a] Bari Wulan,[b]* Song Chen,[a] Jing Wang[a] and Yuanyuan Feng[a]*

[a]*Key Laboratory of Catalytic Conversion and Clean Energy in Universities of Shandong Province, School of Chemistry and Chemical Engineering, Qufu Normal University, Qufu Shandong, 273165, P.R.China.*

[b]*Energy Research Institute, Shandong Key Laboratory of Biomass Efficient Conversion and Utilization, Qilu University of Technology (Shandong Academy of Sciences), Jinan, Shandong, 250014, P. R. China.*

**Correspondence Email: tandx@qfnu.edu.cn, bariwulan@qlu.edu.cn, fengyy@qfnu.edu.cn.*

This PDF file includes:
Experimental Section; Fig. S1 to S15; Table S1.

Experimental Procedures

Computational Method

All spin-polarized DFT calculations were carried out using the Vienna ab initio simulation package (VASP).[1,2] The Perdew-Burke-Ernzerhof (PBE) exchange-correction functional within the generalized gradient approximation (GGA) was employed to describe the exchange-correlation potential.[3,4] The DFT-D3 approach was applied to describe van der Waals (vdW) interactions.[5] A vacuum distance of 20 Å was employed to avoid interactions between periodic images. The cut-off energy of the plane wave basis set was set to 450 eV. The energy and force convergence criteria were set to be 10^{-4} eV and 0.01 eV $Å^{-1}$, respectively. The Brillouin zone was sampled with a 1×1×1 by Gamma centered grids. Based on the experimental results, a three-layer slab repeated in a p(3×4) NiMoN (100) supercell was built as NiMoN. The B-NiMoN, P-NiMoN and S-NiMoN were constructed by utilizing B, Pand S to replace some of the N atoms in the NiMoN. The adsorption energy (E_{ads}) of the adsorbed *OH_2 on the NiMoN, B-NiMoN, P-NiMoN or S-NiMoN is expressed by $E_{ads} = E_{total} - E_{H_2O} - E_{catalyst}$, in which E_{total}, E_{H_2O}, and $E_{catalyst}$ denote the total energies of the adsorbed *OH_2, the isolated H_2O, and the NiMoN, B-NiMoN, P-NiMoN or S-NiMoN, respectively.

Pretreatment Nickel Foam (NF)

The NF substrate was cleaned with acetone and hydrochloric acid solution (3 mol L^{-1}) in an ultrasonic bath for 0.5 h to remove surface organics and oxides; then, the NF substrate was washed with ethanol and excess deionized waterseveral times.

Preparation of NiMoN

In a typical preparation process, 0.3872 g ammonium molybdate tetrahydrate and nickel nitrate hexahydrate were dissolved into 30 mL of ultrapure water. The mixture was then vigorously stirred at room temperature for 2 h to form a homogeneous precursor solution. Next, the solution was transferred into a Teflon liner stainless-steel autoclave, then a piece of treated NF (2×3 cm^2) was immersed in the mixed solution and the autoclave was sealed and heated at 150 °C for 12 h. After the autoclave cooled to room temperature, the as-prepared sample was washed with ethanol and dried in a vacuum oven at 80 °C for 24 h. The solid was annealed in tube furnace at 500 °C in NH_3 atmosphere for 2 h with a heating rate of 5 °C min^{-1}.

Preparation of B-NiMoN, P-NiMoN and S-NiMoN

The preparation process of B-NiMoN, P-NiMoN and S-NiMoN were similar with NiMoN, except that boric acid, disodium hydrogen phosphate, and thiourea were additionally added during the synthesis process, respectivity.

Characterization

The microstructure and morphology of catalysts were characterized by field emission scanning electron microscopy (FESEM, Zeiss Sigma 300), transmission electron microscope (TEM, JEOL JEM-1011 and JEOL JEM-2100F). The crystalline structures information was analyzed on X-ray diffraction (XRD, Bruker D8 diffractometer) with Cu Kα radiation (λ = 0.15418 nm). The X-ray photoelectron spectroscopy (XPS) was carried out with a multipurpose X-ray photoemission spectroscope (Thermo Scientific ESCALAB 250Xi).

Fabrication of Pt/C and RuO_2 electrodes

The Pt/C and RuO_2 electrodes were prepared by loading samples suspension onto NF. Briefly, the Pt/C, RuO_2 and 10 μL Nafion D-521 dispersion were dispersed in absolute ethanol and ultrasonicated for 1 h to form uniform suspension, and the suspension was loaded on the NF, respectively. The electrode was dried in a vacuum oven at 80 °C for 6 h before electrochemical experiment.

Electrochemical Test

A CHI760E electrochemical analyzer (Shanghai Chenhua instrument co. LTD, China) was used in all the electrochemical experiments. All electrochemical experiments were carried out in the three electrodes system. The reference and counter electrodes are Hg/HgO and graphite rod, respectively. All experiments were measured at atmospheric pressure and room temperature. All working electrodes were used for electrochemical experiments with a fixed working area of 0.25 cm^2. Before electrochemical testing, the working electrodes were activated by cyclic voltammetry of 50 sweep segments in electrolyte to generate stable active species. Linear Sweep Voltammetry (LSV) was performed in 1.0 M KOH with/without 0.5 M methanol solution. All potentials reported in this paper are with respect to reversible hydrogen electrode (RHE), which were converted by Equation 1.

Potential in RHE= Applied potential vs Hg/HgO + 0.098 + 0.0592pH (Equation 1).

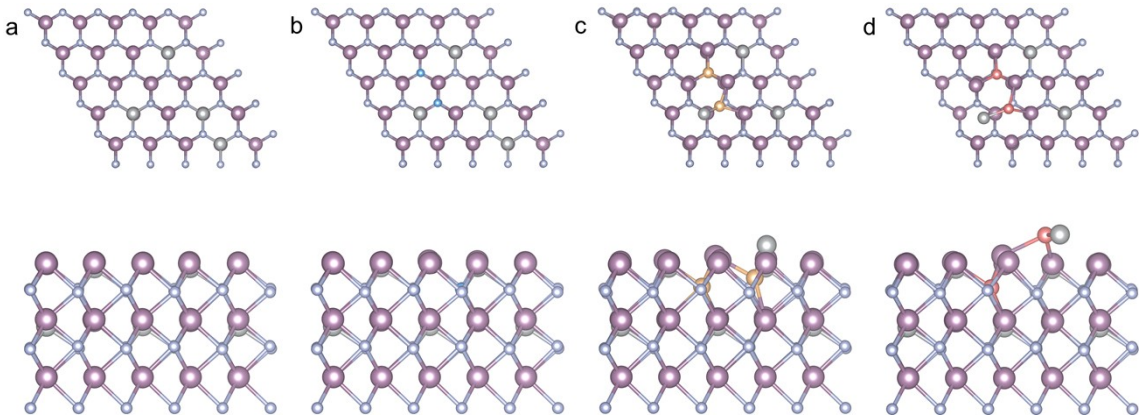

Fig. S1 The optimal structures of (a) NiMoN, (b) B-NiMoN, (c) P-NiMoN and (d) S-NiMoN.

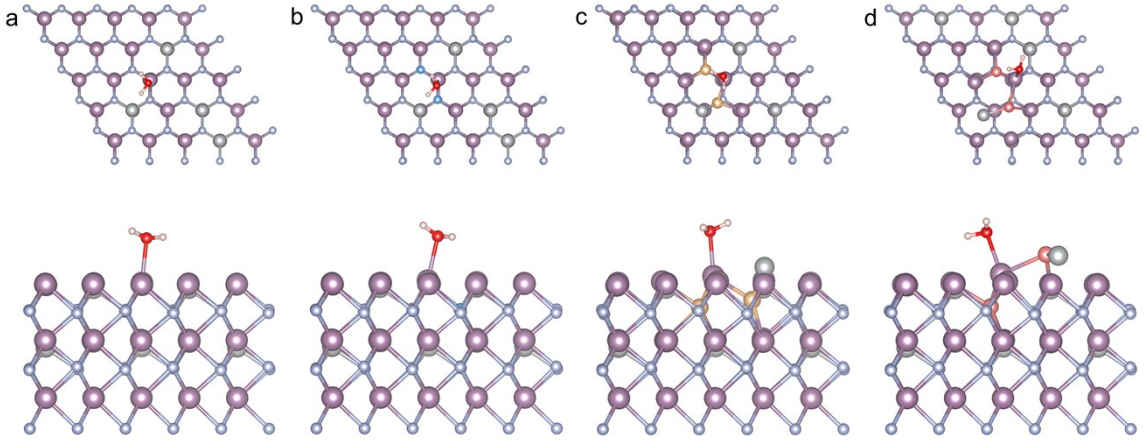

Fig. S2 The optimal structures of H_2O adsorption on (a) NiMoN, (b) B-NiMoN, (c) P-NiMoN and (d) S-NiMoN.

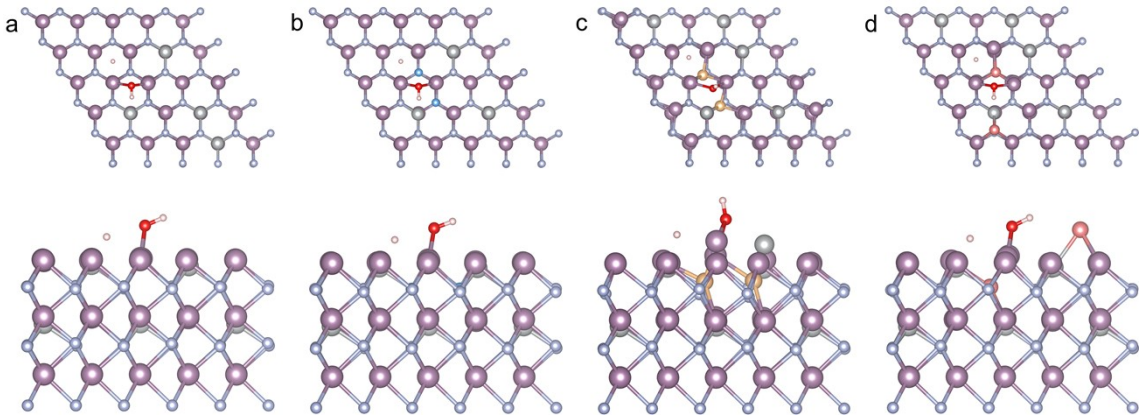

Fig. S3 The optimal structures of H_2O dissociation on (a) NiMoN, (b) B-NiMoN, (c) P-NiMoN and (d) S-NiMoN.

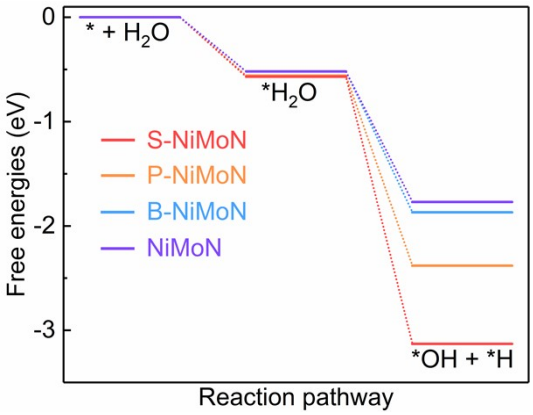

Fig. S4 Free energy diagrams for reducing H_2O into *H and *OH on the surface of NiMoN, B-NiMoN, P-NiMoN and S-NiMoN.

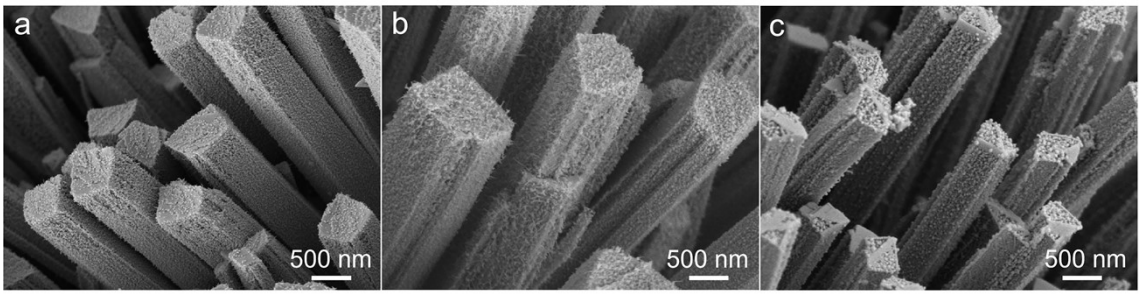

Fig. S5 SEM images of (a) NiMoN, (b) B-NiMoN, (c) P-NiMoN.

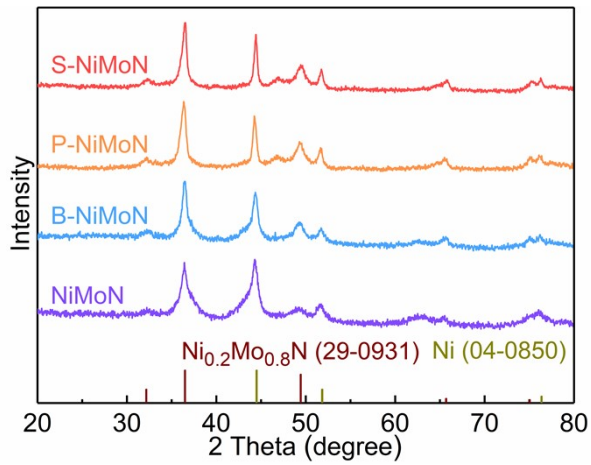

Fig. S6 XRD patterns of NiMoN, B-NiMoN, P-NiMoN and S-NiMoN.

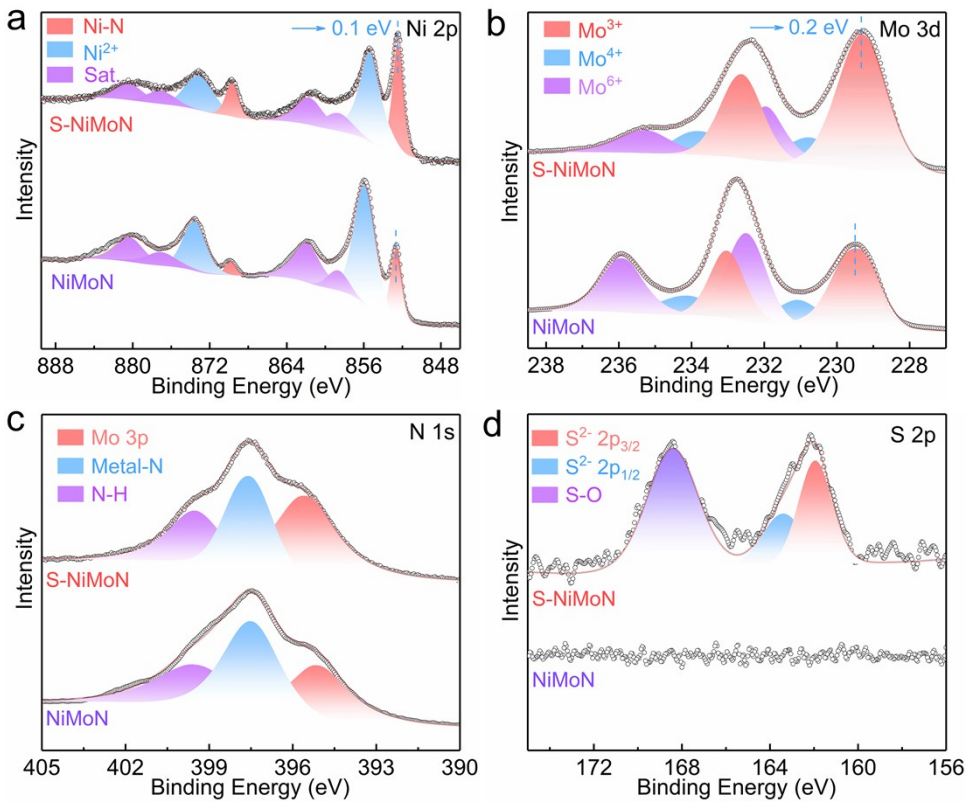

Fig. S7 High-resolution XPS spectra of (a) Ni 2p, (b) Mo 3d, (c) N 1s and (d) S 2p of S-NiMoN and NiMoN.

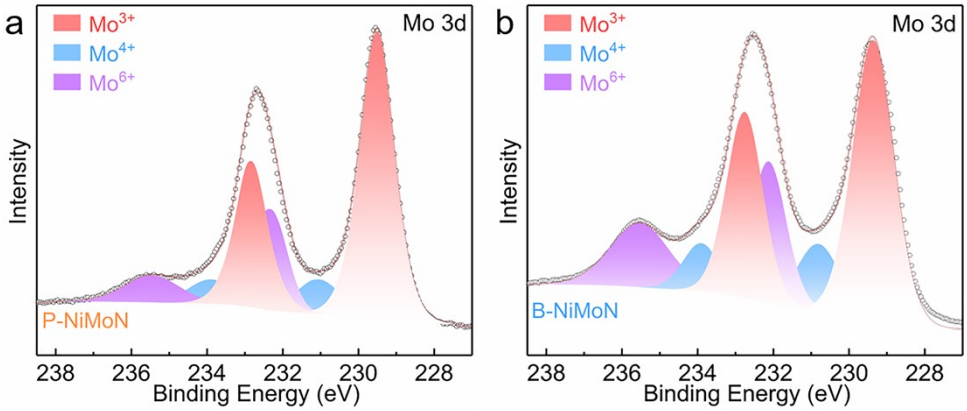

Fig. S8 High-resolution XPS spectra of Mo 3d for (a) P-NiMoN and (b) B-NiMoN.

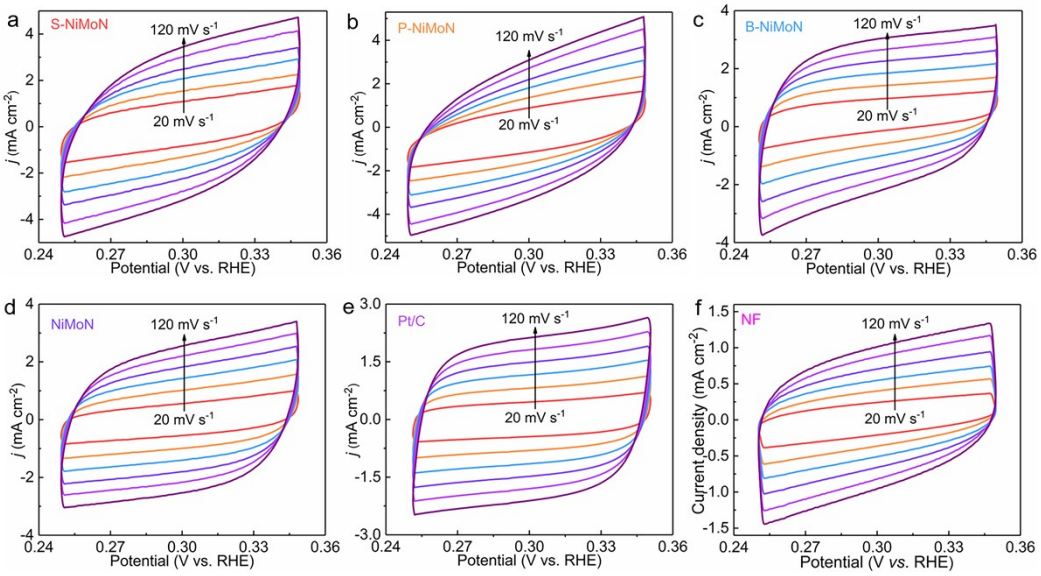

Fig. S9 CV curves acquired at various scan rates in 1.0 M KOH solution of (a) S-NiMoN, (b) P-NiMoN, (c) B-NiMoN, (d) NiMoN, (e) Pt/C and (f) NF.

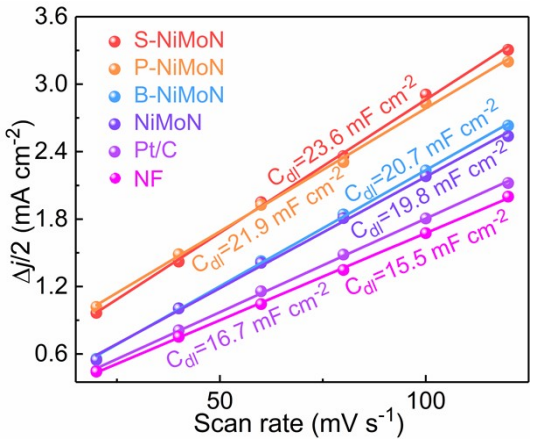

Fig. S10 The the double-layer capacitances of the catalysts and commercial Pt/C.

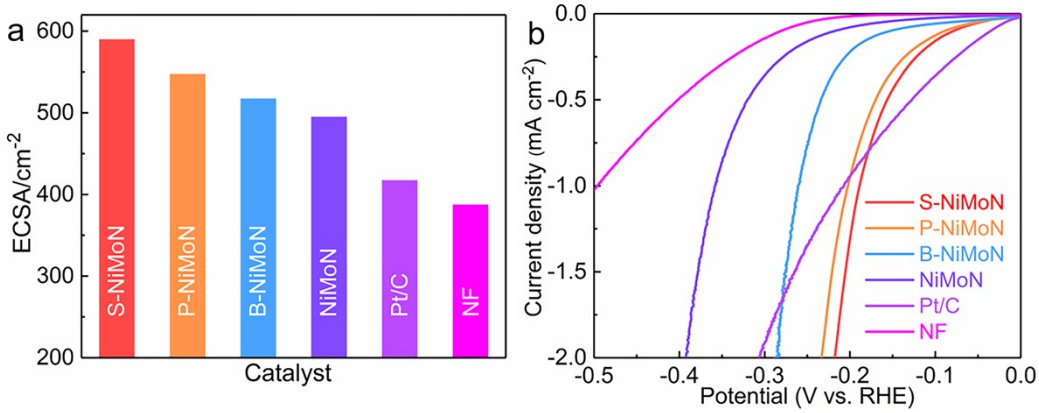

Fig. S11 (a) The electrochemical active areas and (b) HER polarization curves normalized by ECSA of S-NiMoN, P-NiMoN, B-NiMoN, NiMoN and Pt/C.

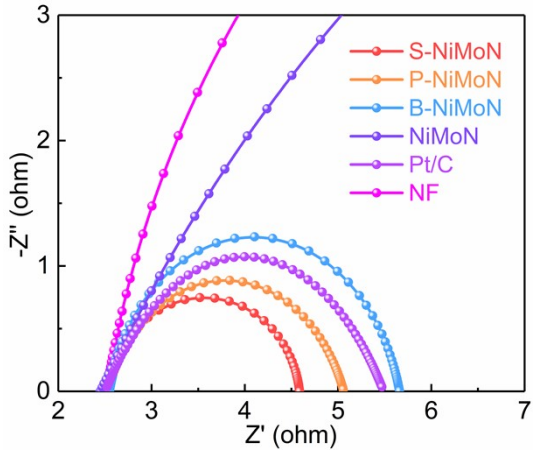

Fig. S12 Nyquist plots of the catalysts and commercial Pt/C.

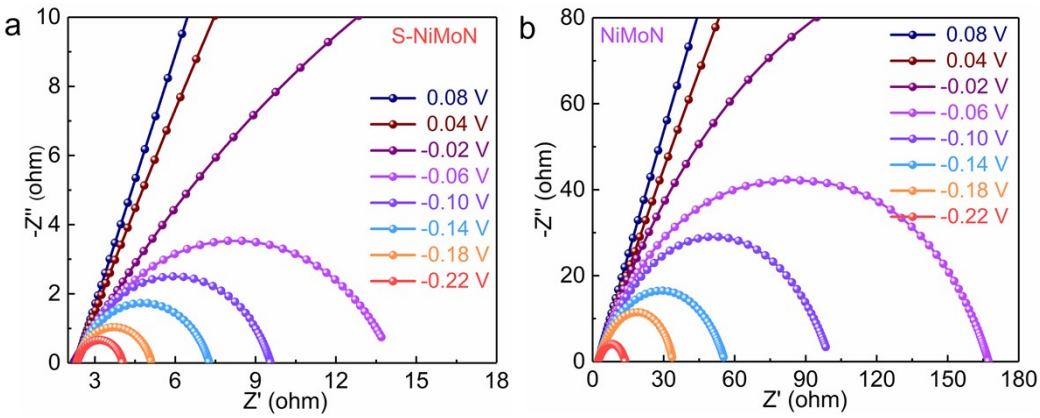

Fig. S13 The potential-dependent Nyquist plots of (a) S-NiMoN and (b) NiMoN for HER.

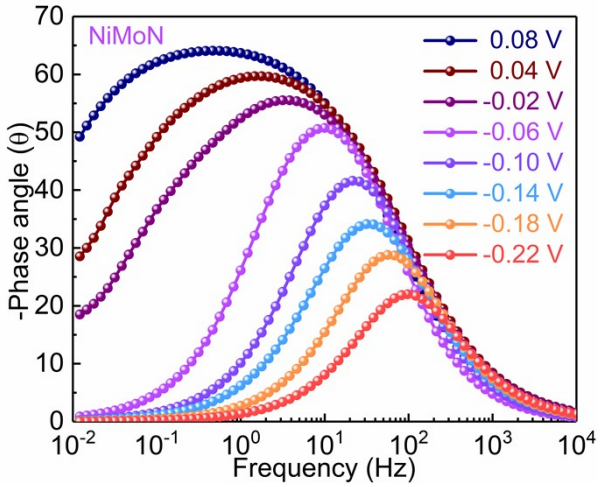

Fig. S14 The potential-dependent Bode plots of NiMoN for HER.

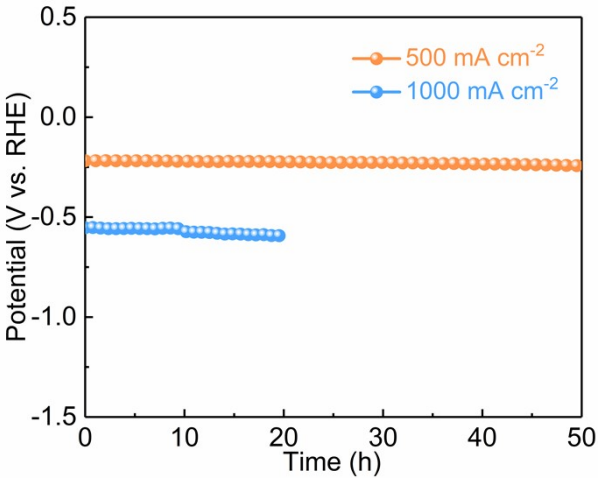

Fig. S15 Stability testing of the S-NiMoN at current densities of 500 and 1000 mA cm^{-2}.

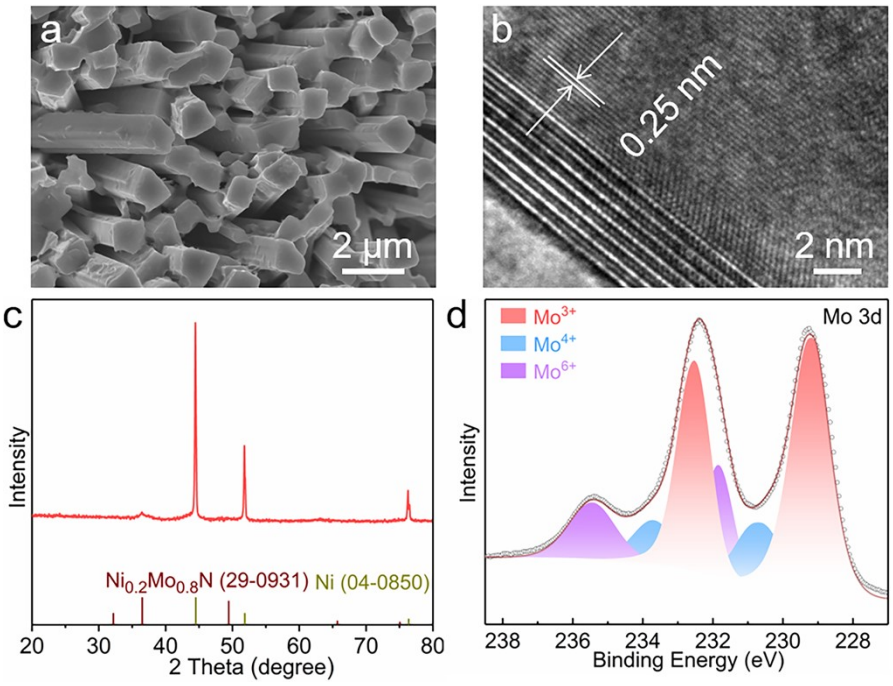

Fig. S16 (a) SEM image, (b) HRTEM image, XRD pattern and (c) high-resolution XPS spectra of Mo 3d for S-NiMoN after stability testing.

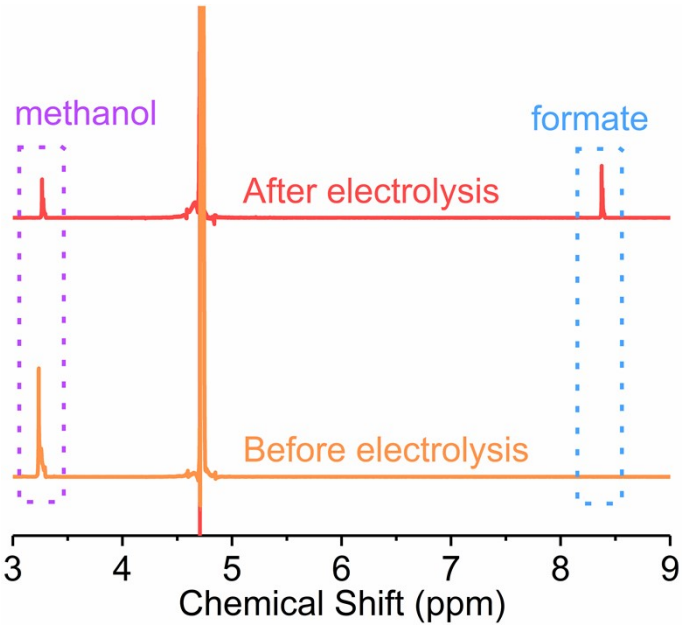

Fig. S17 ^{1}H NMR spectra of the electrolyte for S-NiMoN before and after MOR.

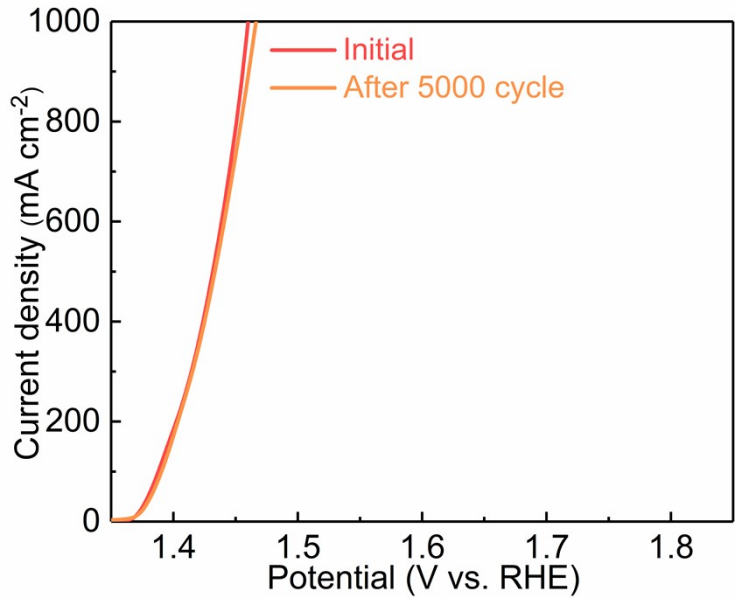

Fig. S18 Polarization curves of S-NiMoN for MOR before and after 5000 cycles.

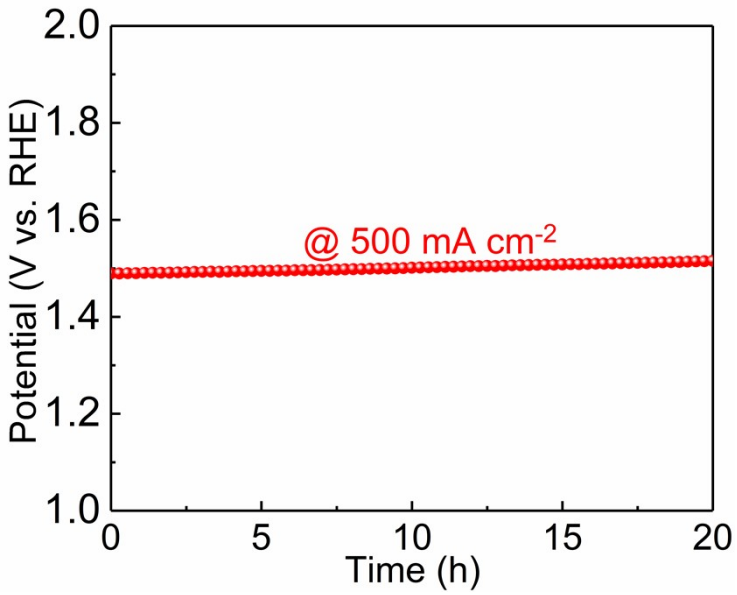

Fig. S19 Chronoamperometry curve at 500 mA cm^{-2} of S-NiMoN for MOR.

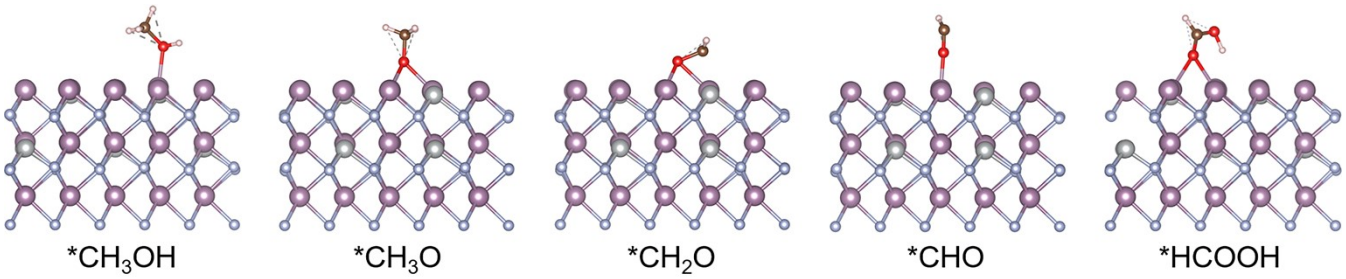

Fig. S20 Geometric configurations of the key intermediates for MOR on NiMoN.

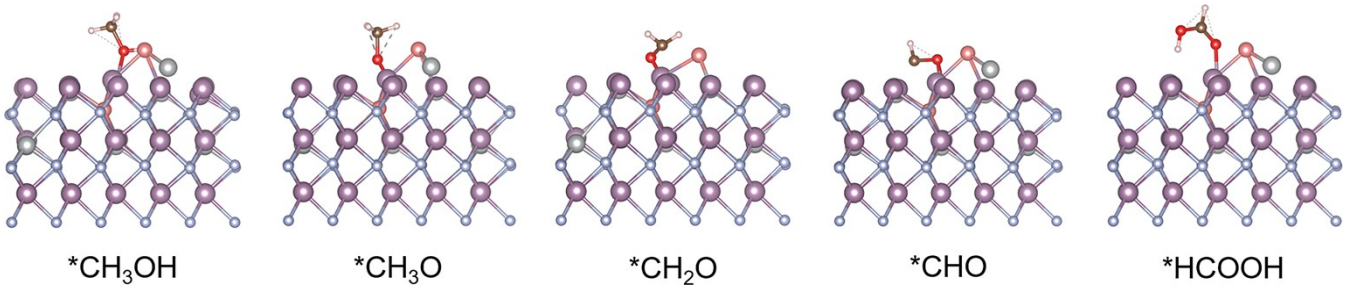

Fig. S21 Geometric configurations of the key intermediates for MOR on S-NiMoN.

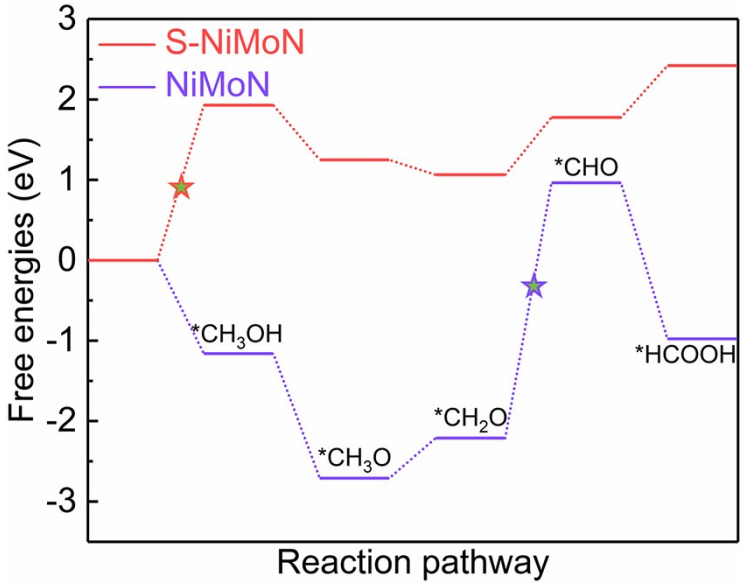

Fig. S22 Gibbs free energy diagram of the MOR on the surface of S-NiMoN and NiMoN.

Table S1 Comparison of the HER activity of S-NiMoN with other published electrocatalysts.

Catalyst	Current density (mA cm^{-2})	Overpotential (mV)	Reference
S-NiMoN	100	104	This work
	500	182	
	1000	211	
$Ni_{0.2}Mo_{0.8}N$/F,N-C	100	83	6
	500	204	
	1000	281	
MnO-CoP/NF	100	94.5	7
	500	186.2	
	1000	259.5	
Cu-FeOOH/Fe_3O_4	100	129	8
	500	285	
	1000	349	
Ni_3S_2/Cr_2S_3@NF	100	160	9
	500	207	
	1000	267	
NMFSOH	100	128	10
	500	175	
	1000	200	
Pt_{NC}/NiMn-MOF	100	44	11
	500	84	
	1000	129	
$FeWO_4$-Ni_3S_2/NF	1000	343	12

Ni_2P−$NiMoO_x$/NF	500	297	13
Ru/CoP	500	187	14
NMB-650	500	200	15
	1000	253	
Mo-Ni_2P-$Ni_{12}P_5$-V_P/NF	500	172	16
NFM-OV_R/NF	500	207	17
	1000	234	
Ni@NCW	500	381	18
	1000	401	
MoO_3/Mo-NiP/NF	500	290	19
$NiSe_2$-Ni_5P_4	500	270	20
Ru-Ni_2P/Fe_2P	500	231	21

References

1 G. Kresse and J. Furthmüller, *Phys. Rev. B*, 1996, **54**, 11169−11186.

2 G. Kresse and J. Hafner, *Phys. Rev. B*, 1993, **47**, 558−561.

3 J. Perdew, K. Burke and M. Ernzerhof, *Phys. Rev. Lett*., 1996, **77**, 3865−3868.

4 P. Blöchl, *Phys. Rev. B*, 1994, **50**, 17953−17979.

5 S. Grimme, J. Antony, S. Ehrlich and H. Krieg, *J. Chem. Phys*., 2010, **132**, 154104.

6 D. Tan, X. Yin, J. Wang, Z. Zhang, X. Zhu, H. Kang and Y. Feng, *J. Mater. Chem. A,* 2025, **13**, 267-274.

7 Y. Dong, Z. Deng, H. Zhang, G. Liu and X. Wang, *Nano Lett.*, 2023, **23**, 9087-9095.

8 C. Yang, W. Zhong, K. Shen, Q. Zhang, R. Zhao, H. Xiang, J. Wu, X. Li and N. Yang, *Adv. Energy Mater.,* 2022, **12**, 2200077.

9 H. Fu, M. Zhou, P. Liu, P. Liu, H. Yin, K. Sun, H. Yang, M. Al-Mamun, P. Hu, H. Wang and H. Zhao, *Journal of the American Chemical Society*, 2022, **144**, 6028-6039.

10 P. Fang, M. Zhu, J. Liu, Z. Zhu, J. Hu and X. Xu, *Adv. Energy Mater.,* 2023, **13**, 2301222.

11 H. Sun, Z. Luo, M. Chen, T. Zhou, B. Wang, B. Xiao, Q. Lu, B. Zi, K. Zhao, X. Zhang, J. Zhao, T. He, J. Zhang, H. Cui, F. Liu, C. Wang, D. Wang and Q. Liu, *ACS Nano*, 2024, **18**, 35654-35670.

12 Z. Wang, G. Qian, T. Yu, J. Chen, F. Shen, L. Luo, Y. Zou and S. Yin, *Chem. Eng. J.,* 2022, **434**, 134669.

13 J. Ren, L. Chen, H. Wang, W. Tian, X. Song, Q. Kong and Z. Yuan, *ACS Catal.*, 2023, **13**, 9792-9805.

14 K. Ji, S. Wang, S. Yao, Y. Ji, G. Wang, W. Ren, J. Wang, F. Zhang, J. Xie, Z. Yang and Y. Yan, *Energy Environ. Sci.,* 2025, **18**, 4764-4774.

15 M. Rafiq, K. Harrath, M. Feng, R. Li, A. Woldu, P. Chu, L. Hu, F. Lu and X. Yao, *Adv. Energy Mater.,* 2024, **14**, 2402866.

16 S. Fan, G. Yang, Y. Jiao, Y. Liu, J. Wang, H. Yan and H. Fu, *Adv. Mater.,* 2025, **37**, 2502523.

17 L. Xiao, C. Cheng, T. Yang, J. Zhang, Y. Han, C. Han, W. Lv, H. Tan, X. Zhao, P. Yin, C. Dong, H. Liu, X. Du and J. Yang, *Adv. Mater.,* 2024, **36**, 2411134.

18 D. Li, H. Cheng, X. Hao, G. Yu, C. Qiu, Y. Xiao, H. Huang, Y. Lu and B. Zhang, *Advanced Materials*, 2024, **36**, 2304917.

19 J. Nie, J. Shi, L. Li, M. Xie, Z. Ouyang, M. Xian, G. Huang, H. Wan, W. Hu and W. Huang, *Adv. Energy Mater.,* 2025, **15**, 2404246.

20 J. Jiang, G. Xu, B. Gong, J. Zhu, W. Wang, T. Zhao, Y. Feng, Q. Wu, S. Liu and L. Zhang, *Adv. Funct. Mater.,* 2025, **35**, 2412685.

21 X. Li, T. Wu, N. Li, S. Zhang, W. Chang, J. Chi, X. Liu and L. Wang, *Adv. Funct. Mater.,* 2024, **34**, 2400734.